Prediction of Elastic Properties of a Poly(styrene−butadiene−styrene) Copolymer Using a Mixed Finite Element Approach

Stephan A. Baeurle,*,†,‡ Glenn H. Fredrickson,‡ and Andrei A. Gusev†

Department of Materials, Institute of Polymers, ETH-Zentrum, CH-8092 Zürich, Switzerland, and Department of Chemical Engineering & Materials, University of California, Santa Barbara, California 93106

Received October 9, 2003; Revised Manuscript Received May 4, 2004

ABSTRACT: Despite several decades of research, the nature of linear elasticity in microphase-separated copolymers with chemically connected glass−rubber phases is still not fully understood. In this paper we investigate the linear elastic properties of a poly(styrene-butadiene-styrene) triblock copolymer using a mixed finite element approach. The technique permits phases of full incompressibility as well as phases of near incompressibility as they occur in this two-component system to be dealt with. Strikingly and contrary to the common belief, we find that the continuum description is accurate and that no additional detailed molecular information is needed to reproduce the available linear elastic experimental data. Our investigation indicates that the anomalous Poisson ratio of the polybutadiene phase of 0.37, determined by previous authors and attributed to molecular characteristics of the polybutadiene phase, might be related to sample end effects arising in their tensile and torsional experiments. We also test the suitability of several semiphenomenological models in reproducing the experimental measurements. We find that some of the methods provide reliable results of accuracy comparable to results from our mixed finite element approach.

1. Introduction

It has long been a goal of polymer science to develop theoretical methods for predicting the physical properties of polymer systems from the knowledge of a few input parameters. The need for such predictions becomes increasingly important as new catalysts are now available that can produce many new exciting architectures.[1−4]

The triblock copolymer poly(styrene-butadiene-styrene) (SBS) is a microphase-separated polymer that has gained widespread use as a thermoplastic elastomer. It is a hard rubber that is used, e.g., for the soles of shoes, tire treads, and other applications where durability is important. For high molecular weights and at low temperatures, the blocks are thermodynamically incompatible, causing the system to phase separate into domains rich in either one of the components. The blocks are covalently bonded together, restricting the phase separation to the order of the radii of gyration of the copolymer blocks, i.e., usually about 100 Å. The equilibrium-phase-separated morphology depends primarily on the bulk polymer composition. Depending on the volume fraction of each block present, the two-phase structure may be periodically arranged in spherical or cylindrical domains of one component in a continuous matrix of the other component or a lamellar structure in which the two components alternate.[5] The mechanical and flow properties of SBS are strongly dependent on the material's morphology.

Because of its technological relevance, extensive efforts have been invested to study its mechanical properties experimentally.[6−9] However, still only little is known about the morphological changes in the system under stress, which involves an interplay of the polystyrene (PS) and polybutadiene (PB) phases. For example, a particularly interesting, as yet unsolved, question is the contribution of the confined PB phase to the overall mechanical behavior of SBS. In preceding works[7,9] the rubbery phase was interpreted to have an unexpectedly low bulk modulus, which is in opposition to the usual assumption for rubber materials. Accordingly, one had to assume a rather untypical Poisson ratio of 0.37 for the PB phase, to reproduce the experimentally determined angular dependence of the effective Young modulus with semiphenomenological theories of fiber reinforcement. This unusual finding was explained with the argument that the PB bridging chains between the PS blocks might be too short and not sufficiently entangled for "classical" rubber-like behavior.

In this work we analyze the problem using the finite element route and investigate the effectiveness of the continuum approach for this class of nanostructured materials. In this way we aim to elucidate the role of the PB bridging chains in the overall mechanical behavior of this triblock copolymer and to check the validity of several semiphenomenological theories employed by previous authors. In fact, it is worth considering that the rigorous upper/lower variational bounds are known to be wide for systems where the bulk and shear moduli of the components differ significantly, while the semiphenomenological theories are typically not accurate in principle; i.e., they rely on some approximation(s). Moreover, these theories have originally been designed for composites with inclusions embedded in ordinary solid matrices with Poisson ratios < 0.4. On the contrary, the finite element route is accurate in principle; i.e., in the limit of an infinite number of elements the predictions should become exact. Within this approach, however, it is important to take into account that each small portion of the rubbery phase tends to preserve volume under deformation, i.e., that such a medium is nearly *incompressible* characterized

† ETH-Zentrum.
‡ University of California.

10.1021/ma035528d CCC: $27.50
Published on Web 06/25/2004

by a Poisson ratio close to $\nu = 0.5$. A well-known difficulty in handling incompressible media with finite element methods is that the standard displacement formulation of elastic problems fails and, typically, leads to highly oscillatory results when the simple linear approximation with triangular elements is used.[10] In practice, the problems already arise when the material is nearly incompressible with $\nu > 0.4$. To overcome the difficulty, we apply the mixed finite element (MFE) approach to the SBS system mentioned previously using a two-field formulation, where the displacement $\mathbf{u}$ and the pressure p are the free variables of the problem. Such a formulation allows the treatment of fully incompressible phases as well as nearly incompressible ones as they occur in the two-component system considered in this work.

Our paper is organized as follows. In section 2 we give a brief review of the MFE approach, followed in section 3 by a description of the mechanical aspects of the model considered herein as well as an introduction of the semiphenomenological theories of fiber reinforcement. In section 4 we present and discuss the results in comparison to the theoretical approaches introduced previously and to the experimental results. Finally, we end the paper with the conclusions and a brief outlook.

2. Theory

The material flow of a system in static equilibrium is described by the principle of linear momentum conservation:[11]

$$\nabla\cdot\boldsymbol{\sigma} + \mathbf{f} = 0 \quad \text{in domain } \Omega \tag{1}$$

where $\boldsymbol{\sigma}$ and $\mathbf{f}$ represent the stress tensor and body force per unit volume, respectively. This equation has to be solved simultaneously with an appropriate constitutive equation and the following boundary conditions:

$$\begin{aligned} \boldsymbol{\sigma}\cdot\mathbf{n} &= \bar{\mathbf{t}} \quad \text{on boundary } \Gamma_t \\ \mathbf{u} &= \bar{\mathbf{u}} \quad \text{on boundary } \Gamma_u \end{aligned} \tag{2}$$

where $\mathbf{u}$ is the vector of displacement and $\mathbf{n}$ the unit vector normal to the surface Γ_t. The vector $\bar{\mathbf{t}}$ is a distributed external loading acting on it. The constitutive stress−strain relation for a linear isotropic elastic deformation can be expressed as[11]

$$\boldsymbol{\sigma} = 2G\epsilon^{\mathrm{d}} - K\epsilon_{\mathrm{v}}\mathbf{I} \tag{3}$$

where ϵ^{d} and $\mathbf{I}$ represent the deviatoric strain and identity tensor, respectively. Moreover, ϵ_{v} denotes the volumetric strain, while G and K represent the shear and bulk moduli, respectively. The deviatoric strain tensor is defined as

$$\epsilon^{\mathrm{d}} = \epsilon - (1/3)\mathbf{m}\epsilon_{\mathrm{v}} \tag{4}$$

where ϵ is the strain tensor and

$$\epsilon_{\mathrm{v}} = \nabla\cdot\mathbf{u} = \mathbf{m}^{\mathrm{T}}\epsilon \quad \text{in } \Omega \tag{5}$$

The matrix $\mathbf{m}$ denotes the equivalent of the tensorial Kronecker δ given by $\mathbf{m} = [1, 1, 1, 0, 0, 0]^{\mathrm{T}}$.[12] As the Poisson ratio ν approaches 0.5, resistance to volume change is greatly increased assuming resistance to shearing remains constant. This can easily be seen by calculating the ratio $K/G = 2(1 + \nu)/3(1 - 2\nu)$, which approaches infinity as $\nu \rightarrow 0.5$. This limit creates a problem in the constitutive eq 3. A possibility to circumvent it is to rewrite the problem in a new formulation where the hydrostatic pressure p is considered as an independent unknown, in addition to the displacement field $\mathbf{u}$. For isotropic deformations the pressure is related to the volumetric strain through the bulk modulus of the material, i.e.

$$p/K = \epsilon_{\mathrm{v}} \quad \text{in } \Omega \tag{6}$$

Taking into account the previous equation, we can easily see that in the incompressible case eq 5 changes into $\nabla\cdot\mathbf{u} = 0$, if the pressure is finite. This definition of the pressure provides us a condition which must be fulfilled at all times. The boundary-value problem to be solved can thus be summarized as follows:

$$\begin{aligned} \nabla\cdot\boldsymbol{\sigma} + \mathbf{f} &= 0 \quad \text{in } \Omega \\ p/K + \nabla\cdot\mathbf{u} &= 0 \quad \text{in } \Omega \\ \boldsymbol{\sigma}\cdot\mathbf{n} &= \bar{\mathbf{t}} \quad \text{on } \Gamma_{\mathrm{t}} \\ \mathbf{u} &= \bar{\mathbf{u}} \quad \text{on } \Gamma_{\mathrm{u}} \end{aligned} \tag{7}$$

with the constitutive relation

$$\boldsymbol{\sigma} = 2G[\epsilon - (1/3)\mathbf{m}\nabla\cdot\mathbf{u}] - p\mathbf{I} \tag{8}$$

Note that we have employed eqs 4−6 to rewrite the constitutive relation 3. We recognize that in the new formulation the displacement $\mathbf{u}$ and the pressure p are now the two unknown variables of the problem.

The virtual work principle is used to establish the equilibrium condition, treating p as an independent variable. This results in[10]

$$\int_\Omega \delta\epsilon^{\mathrm{T}}\mathbf{D}_{\mathrm{d}}\epsilon \, \mathrm{d}\Omega + \int_\Omega \delta\epsilon^{\mathrm{T}}\mathbf{m}p \, \mathrm{d}\Omega - \int_\Omega \delta\mathbf{u}^{\mathrm{T}}\mathbf{b} \, \mathrm{d}\Omega - \int_{\Gamma_t} \delta\mathbf{u}^{\mathrm{T}}\bar{\mathbf{t}} \, \mathrm{d}\Gamma_t = 0 \tag{9}$$

where $\mathbf{b}$ represents a distributed body force, while

$$\mathbf{D}_{\mathrm{d}} = 2G(\mathbf{I}_0 - (1/3)\mathbf{m}\mathbf{m}^{\mathrm{T}}) \tag{10}$$

is a deviatoric form of the elastic moduli with $\mathbf{I}_0$ a diagonal matrix of constants (for definitions of deviatoric forms see appendix A). In addition, we impose a weak form of eq 6, i.e.

$$\int_\Omega \delta p[\mathbf{m}^{\mathrm{T}}\epsilon - p/K] \, \mathrm{d}\Omega = 0 \tag{11}$$

with $\epsilon = \mathbf{S}\mathbf{u}$, where $\mathbf{S}$ is a suitable linear 6×3 strain-displacement-operator matrix. The independent approximation of $\mathbf{u}$ and p, i.e., $\mathbf{u} \approx \hat{\mathbf{u}} = \mathbf{N}_{\mathbf{u}}\tilde{\mathbf{u}}$ and $p \approx \hat{p} = \boldsymbol{N}_{\mathbf{p}}\tilde{\mathbf{p}}$, then finally provides the mixed formulation of the problem

$$\begin{bmatrix} \mathbf{A} & \mathbf{C} \\ \mathbf{C}^{\mathrm{T}} & -\mathbf{V} \end{bmatrix} \begin{Bmatrix} \tilde{\mathbf{u}} \\ \tilde{\mathbf{p}} \end{Bmatrix} = \begin{Bmatrix} \mathbf{f}_1 \\ \mathbf{f}_2 \end{Bmatrix} \tag{12}$$

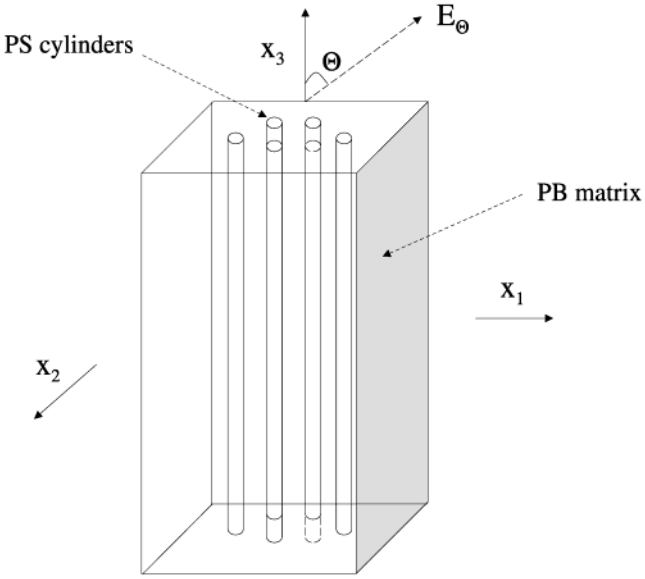

Figure 1. System of hexagonally packed cylinders of PS embedded in a PB matrix.

with

$$\mathbf{A} = \int_\Omega \mathbf{B}^T \mathbf{D}_d \mathbf{B}\, d\Omega$$

$$\mathbf{C} = \int_\Omega \mathbf{B}^T \mathbf{m} \mathbf{N_p}\, d\Omega$$

$$\mathbf{V} = \int_\Omega \mathbf{N_p}^T (1/K) \mathbf{N_p}\, d\Omega \qquad (13)$$

$$\mathbf{f}_1 = \int_\Omega \mathbf{N_u}^T \mathbf{b}\, d\Omega + \int_{\Gamma_t} \mathbf{N_u}^T \bar{\mathbf{t}}\, d\Gamma$$

$$\mathbf{f}_2 = 0$$

where $\mathbf{B} = \mathbf{S}\mathbf{N_u}$ is defined via $\epsilon = \mathbf{S}\mathbf{u} = \mathbf{B}\mathbf{a}$, with $\mathbf{a}$ the nodal displacement vector. Moreover, $\mathbf{N_p}$ and $\mathbf{N_u}$ represent the shape functions of the pressure and displacement field, respectively. We note that for incompressible situations $\mathbf{V} = 0$, and eq 12 goes over in the "standard" block form encountered by solving the Stokes equation. This shows us that the mixed formulation remains useful in the incompressible case.

3. Mechanical Aspects and Theoretical Approaches

The material investigated in this work is a poly(styrene-butadiene-styrene) triblock copolymer with a weight fraction of 25% PS, which corresponds to a volume concentration of $C = 0.2$. The system, visualized in Figure 1, consists of a hexagonally packed array of PS cylinders embedded in a PB matrix, which can be regarded as a miniature fiber-reinforced system.

To predict theoretically its linear elastic properties, it is necessary to determine the independent elastic constants of the model. For a material possessing hexagonal symmetry about the x_3-axis, the compliance tensor is symmetric about the leading diagonal and the five independent compliance components are S_{11}, S_{33}, S_{12}, S_{13}, and S_{44}. S_{11} and S_{22} are, respectively, the compliances along the directions x_1 and x_2, which are transverse to the fiber direction x_3, and they are equal due to symmetry. S_{33} is the component of the compliance tensor along the x_3 direction, while S_{44} is a shear compliance which is directly related to shear modulus G_{SBS} of the model via $S_{44} = 1/G_{SBS}$. For a detailed discussion of the mechanical aspects of the model we refer to ref 7.

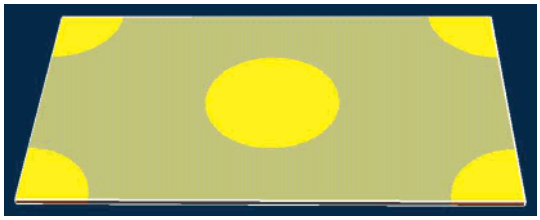

Figure 2. Sketch of the model system employed in our MFE calculations representing a system of hexagonally packed cylinders of PS embedded in a PB matrix.

To investigate the accuracy of the different theoretical approaches, we compare in the following the components of the compliance tensor obtained with MFE to the theoretical as well as experimental results presented by Arridge and Folkes in ref 7. Moreover, we compare the orientation-dependent compliance

$$S_{33}' = 1/E_\theta = S_{11} \sin^4\theta + (2S_{13} + S_{44}) \sin^2\theta \cos^2\theta + S_{33} \cos^4\theta \qquad (14)$$

where the angle θ is defined as in Figure 1. It is worth noting that S_{11} and S_{33} are related to the Young moduli E_{90} and E_0 via $E_{90} = 1/S_{11}$ and $E_0 = 1/S_{33}$, respectively.

In our MFE calculations we use a serendipity family brick element with a linear interpolation of the displacement and a discontinuous interpolation of the pressure degrees of freedom. We apply the system strain by changing the size and the shape of the periodic computational cell.[13,14] We calculate the effective elastic constants from the linear response equation relating the volume-averaged local stress and the applied system strain. We perform six independent optimization runs, to calculate the complete set of effective elastic constants, and use an iterative preconditioned conjugate residual solver. As a stopping criterion, we employ a 10^{-4} reduction in the first residual norm. In the calculations we employ the model system, visualized in Figure 2, consisting of a grid of $100 \times 173 \times 2$ elements (1.4×10^5 degrees of freedom) and impose periodic boundary conditions. The grid is found to reproduce the composite microstructure and thus the effective elastic constants accurately. On a 2.5 GHz Pentium 4 computer, the six optimization runs with such a system take on average about 30 CPU min.

For comparison we select the theories of fiber-reinforced materials for hexagonal symmetry employed by Arridge and Folkes in the same reference.[7] In this work the following methods have been considered.

(1) The modified series−parallel model developed by Folkes and Keller[6] considers series and parallel arrangements of elements of differing stiffness and assumes infinitely rigid PS cylinders. It relies on a two-phase polymer model developed by Takayanagi et al., commonly used in polymer research.[15] The method provides reliable values for the longitudinal Young modulus, but is inaccurate for the other elastic constants.

(2) The self-consistent model method of Whitney and Riley[16] uses a simple unit-cell model consisting of a single filament embedded in a matrix cylinder of finite outer radius, to derive equations for the Young moduli along the fiber direction and transverse to it. The method consists of determining the stresses in the

cylinders for various surface loadings and, subsequently, using the results in an energy balance.

(3) The variational method of Hashin and Hill[17,18] relies on an extension of the work of Hashin and Rosen.[19] It employs the energy theorems of classical elasticity, to obtain upper and lower bounds for the five elastic constants. The minimum complementary energy theorem yields the lower bound, while the minimum potential energy theorem yields the upper bound. Hill[18] showed by formal and physical arguments that these are the best bounds that can be obtained without taking into account detailed local geometry and that the rule of mixtures gives the lower bound for the Young modulus in the fiber direction E_0.

(4) The variational method of Rosen[20] is an improvement of the composite cylinder assemblage model proposed in the paper of Hashin and Rosen.[19] This model incorporates randomness in size and structure of the fibers and permits the derivation of simple closed form expressions for the effective elastic moduli.

(5) The exact-calculation method of Van Fo Fy and Savin[21] relies on Fil'shtinskii's approach to handle fiber composite materials.[22] It is based on the solution of the equations of elastic equilibrium using an expansion in elliptic functions, to solve the problem of hexagonal symmetry.

Following the procedure of Arridge and Folkes, we adjust the bulk and shear moduli of the model to match particular experimental compliances and then compare the predicted values of other compliances among the various theories. Within the accuracy of the experimental measurements we will also be able to deduce new information about the material.

4. Results and Discussion

Our MFE method and the theoretical approaches introduced previously require five parameters as input, namely, the concentration of the PS fibers, C, their bulk and shear moduli, K_{PS} and G_{PS}, and the bulk and shear moduli of the PB matrix, K_{PB} and G_{PB}. To analyze the sensitivity of the compliances to the bulk and shear moduli of the PS and PB phases, we perform calculations by varying these parameters in the ranges $G_{PB} = 0.0005-0.0015$ GPa, $K_{PB} = 1.0-2.0$ GPa, $G_{PS} = 0.5-2.0$ GPa, and $K_{PS} = 1.0-2.0$ GPa. These ranges cover the typical ranges of moduli of PB[23,24] and PS,[25-27] which essentially depend on the number of cross-links and the molecular weight of the component. In addition, we perform calculations with a bulk modulus of $K_{PB} = 0.086$ GPa used by Arridge and Folkes,[7,6] which substantially deviates from the bulk moduli of rubber materials.[24] In Figure 3 we plot the transverse compliance S_{11} as a function of G_{PB} and for different values of K_{PB}, G_{PS}, and K_{PS}. We see that this compliance possesses a strong dependence on G_{PB}, but remains unaffected by the variation of the other input parameters. The same conclusions can be drawn for the shear compliance S_{44}, which is shown in Figure 4. Next, we visualize in Figure 5 the compliance S_{33} as a function of G_{PS} and for different values of G_{PB}, K_{PB}, and K_{PS}. We recognize that S_{33} is entirely dominated by the moduli of PS, G_{PS}, and K_{PS}, and is insensitive to the moduli of PB. These observations regarding the compliances can be explained by the large difference in stiffness of PB and PS. It follows that S_{11} and S_{44} on one hand and S_{33} on the other can be separately adjusted to fit the available experimental data.

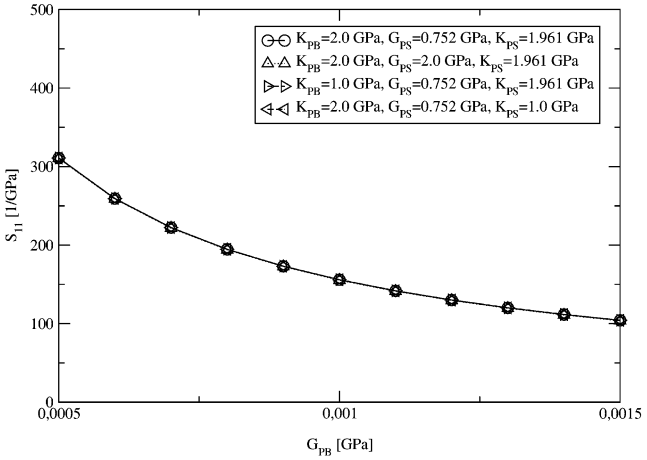

Figure 3. S_{11} compliance for a system of hexagonally packed cylinders of PS in a PB matrix as a function of G_{PB} and for different K_{PB}, G_{PS}, and K_{PS} values.

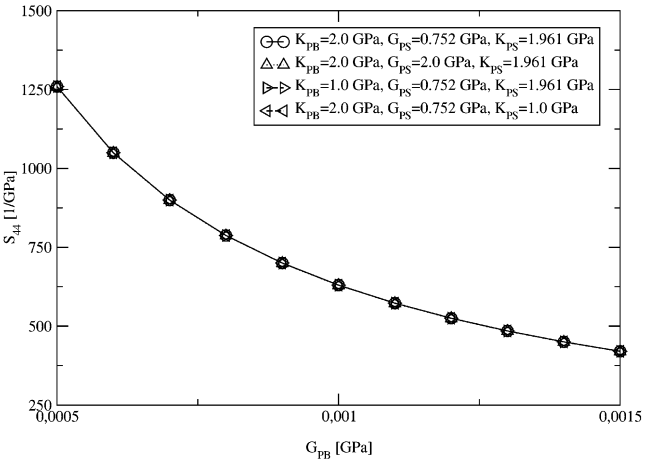

Figure 4. S_{44} compliance for a system of hexagonally packed cylinders of PS in a PB matrix as a function of G_{PB} and for different K_{PB}, G_{PS}, and K_{PS} values.

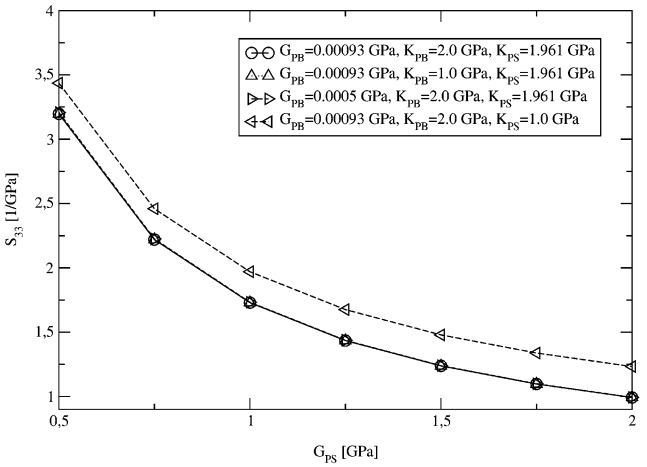

Figure 5. S_{33} compliance for a system of hexagonally packed cylinders of PS in a PB matrix as a function of G_{PS} and for different K_{PS}, G_{PB}, and K_{PB} values.

To investigate the accuracy of the semiphenomenological theories, we additionally perform MFE calculations using the same input parameters as Arridge and Folkes,[7] i.e., $K_{PB} = 0.08618$ GPa, $G_{PB} = 0.00093$ GPa, $K_{PS} = 1.961$ GPa, and $G_{PS} = 0.752$ GPa, where $\nu_{PB} = 0.4946$ and $\nu_{PS} = 0.33$. In Table 1 we list the compliances obtained with our MFE method in comparison to the

Table 1. Compliances from the MFE Method in Comparison to Results Provided by the Theories of Fiber Reinforcement and the Tensile Experiment

method	$S_{11} \times 10^{-3}$ (GPa^{-1})	$S_{33} \times 10^{-1}$ (GPa^{-1})	$(2S_{13} + S_{44}) \times 10^{-3}$ (GPa^{-1})
MFE	0.17	0.21	0.68
Van Fo Fy and Savin	0.18	0.25	0.72
Whitney and Riley	0.10	0.25	0.72
Hashin and Hill upper bound	0.18	0.25	0.72
Hashin and Hill lower bound	0.0054	0.25	0.0012
Rosen	0.14	0.25	0.72
experiment	0.23 ± 0.03	0.24	0.66 ± 0.07

Table 2. Compliances from the MFE Method in Comparison to Results Provided by the Theories of Fiber Reinforcement and the Tensile Experiment[a]

method	$S_{11} \times 10^{-3}$ (GPa^{-1})	$S_{33} \times 10^{-1}$ (GPa^{-1})	$(2S_{13} + S_{44}) \times 10^{-3}$ (GPa^{-1})
MFE	0.16	0.24	0.66
Van Fo Fy and Savin	0.17	0.24	0.66
Whitney and Riley	0.0093	0.24	0.66
Hashin and Hill upper bound	0.17	0.24	0.66
Hashin and Hill lower bound	0.0051	0.23	0.091
Rosen	0.13	0.24	0.66
experiment	0.23 ± 0.03	0.24	0.66 ± 0.07

[a] The compliances $2S_{13} + S_{44}$ and S_{33} are adjusted to the experimental result.

results obtained by Arridge and Folkes using the theories of fiber reinforcement and extensional elasticity measurements. From the table we conclude that in the case of S_{11} the method of Van Fo Fy and Savin and the method of Hashin and Hill (upper bound) provide values similar in accuracy to the values of our MFE method. The deviations from the experimental result amount to 21.7%, 21.7%, and 26.1%, respectively, while for the remaining theories the deviations are much larger. In the case of $2S_{13} + S_{44}$ we see that the MFE value is much closer to the experimental value than the values of the other theories, which is reflected by a deviation of 3% for the former method and 9% for the latter.

To further assess the accuracy of the semiphenomenological theories in comparison to our MFE approach, we proceed in the same way as Arridge and Folkes, which consists of adjusting either S_{11} or $2S_{13} + S_{44}$, thereby eliminating their error, and comparing the remaining compliances with those of experiment. Because in the latter case we know that $S_{13} \ll S_{44}$, the procedure is equivalent to adjusting S_{44}. S_{33} can always be adjusted independently by selecting G_{PS} or K_{PS} suitably. From the results we can then evaluate the orientation-dependent compliance S_{33}' at any angle θ. By fitting $2S_{13} + S_{44}$ to the experimental result, Arridge and Folkes obtained the input parameters $G_{PB} = 0.00101$ GPa, $G_{PS} = 0.797$ GPa, and $K_{PS} = 2.078$ GPa, where $\nu_{PS} = 0.33$, and by assuming a fully incompressible PB matrix, i.e., $\nu_{PB} = 0.5$. Following the same procedure with our MFE approach, we obtained the parameters $G_{PB} = 0.00095$ GPa, $K_{PB} = 2.0$ GPa, $G_{PS} = 0.68$ GPa, and $K_{PS} = 2.0$ GPa, with $\nu_{PS} = 0.33$ and $\nu_{PB} = 0.4998$. All the resulting compliances are listed in Table 2. We can deduce from it that the S_{11} compliance provided by the MFE method very nearly coincides with the result obtained with the method of Van Fo Fy and Savin, as well as the upper bound of Hashin and Hill. The MFE result deviates 30.4% from the experimental value, while the latter methods both provide a deviation of 26.1%. The methods of Rosen and of Whitney and Riley provide much larger deviations, i.e., 43.5% and 96.0%, respectively. To quantify the mechanical anisotropy, we calculate next the S_{33}' compliance using the compliances of the table considered previously. In Figure 6 we show the quantity as a function of the angle θ. We see that the upper bound of Hashin and Hill and the result of the method of Van Fo Fy and Savin are very close to the result provided by our MFE approach, while the method of Rosen and the method of Whitney and Riley provide compliances far below. Next, adjusting the compliance S_{11} to the experimental value gives the results presented in Table 3. We obtained the MFE results using the input parameters $G_{PB} = 0.00069$ GPa, $K_{PB} = 2.0$ GPa, $G_{PS} = 0.68$ GPa, and $G_{PS} = 2.0$ GPa, while Arridge and Folkes did not specify the parameters they employed. The corresponding angular dependence of the compliance S_{33}' is shown in Figure 7. We see that the curves of the method of Van Fo Fy and Savin and of Hashin and Hill (upper bound) are in close vicinity to the curve provided by the MFE method. In contrast, the curves provided by the method of Rosen and the method of Whitney and Riley deviate substantially. In addition, we observe that all these curves at intermediate angular ranges lie outside the error bounds of the tensile experiment.

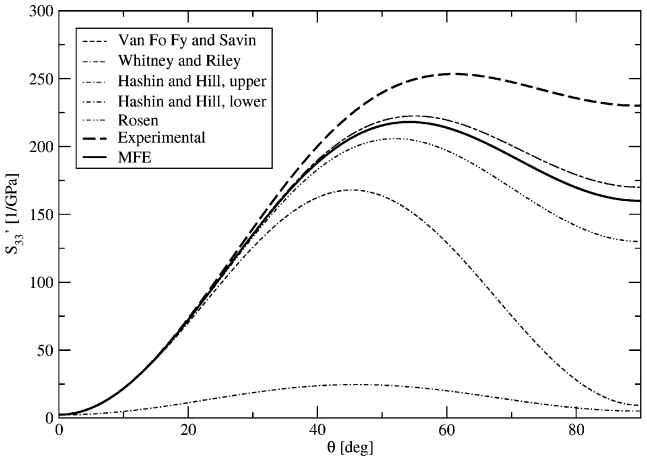

Figure 6. S_{33}' compliance yielded with the MFE method in comparison to the results obtained with the theories of fiber reinforcement and the tensile experiment. The compliances $2S_{13} + S_{44}$ and S_{33} are adjusted to the experimental result.

Table 3. Compliances from the MFE Method in Comparison to Results Provided by the Theories of Fiber Reinforcement and the Tensile Experiment[a]

method	$S_{11} \times 10^{-3}$ (GPa^{-1})	$S_{33} \times 10^{-1}$ (GPa^{-1})	$(2S_{13} + S_{44}) \times 10^{-3}$ (GPa^{-1})
MFE	0.23	0.24	0.91
Van Fo Fy and Savin	0.23	0.24	0.89
Hashin and Hill upper bound	0.23	0.24	0.89
Hashin and Hill lower bound	0.0052	0.23	0.011
Rosen	0.22	0.24	1.1
Simple model	0.23	0.24	
Experimental	0.23 ± 0.03	0.24	0.66 ± 0.07

[a] The compliances S_{11} and S_{33} are adjusted to the experimental result.

To obtain a complete fit to all the experimental compliances, Arridge and Folkes proposed to relax the incompressibility assumption for the PB matrix. According to this procedure we get with the MFE method

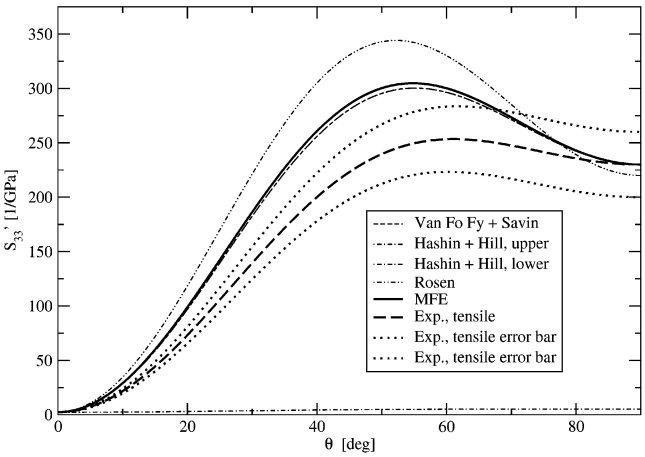

Figure 7. S_{33}' compliance yielded with the MFE method in comparison to the results obtained with the theories of fiber reinforcement and the tensile experiment. The compliances S_{11} and S_{33} are adjusted to the experimental result.

Table 4. Poisson Ratio of the PB Matrix Yielded from the MFE Method in Comparison to Results of the Theories of Fiber Reinforcement and the Tensile Experiment[a]

method	$K_{PB} \times 10^3$ (GPa)	ν_{PB}
MFE	3.0	0.36
Van Fo Fy and Savin	3.6	0.37
Whitney and Riley	2.0	0.28
Hashin and Hill lower bound	3.6	0.37
Rosen	2.8	0.34

[a] All compliances are adjusted to the experimental values.

the Poisson ratio ν_{PB} given in Table 4 using the input parameters $G_{PB} = 0.00095$ GPa, $K_{PB} = 0.003$ GPa, $G_{PS} = 0.68$ GPa, and $K_{PS} = 1.961$ GPa. It is compared with the results of Arridge and Folkes.[7] We conclude from the table that our Poisson ratio is in close agreement with the results obtained with the method of Van Fo Fy and Savin and the lower bound of Hashin and Hill, while the remaining methods provide much smaller values. Moreover, we can also deduce from the corresponding bulk modulus that such a Poisson ratio implies that the PB phase is compressible, which is contrary to the usual assumption for a rubber. Arridge and Folkes explained this result with the argument that the PB chains between the PS blocks might be too short and insufficiently entangled for classical rubber-like behavior.

However, in subsequent works[28−30] the same authors found that the experimental determination of the elastic constants of highly anisotropic materials can be problematic with the conventional test methods, where tension, bending, or torsion is involved. The origin of the error occurring in such measurements relates to sample end effects, which are conventionally taken into account by St. Venant's principle. This principle states that the end effects observed during torsion or tension of the samples die away within a length approximately equal to the maximum cross-sectional dimension. It has largely caused investigators in the past to ignore end effects when making measurements of elastic constants.[30] However, Horgan has demonstrated theoretically that in highly anisotropic materials the decay length can be considerably greater than the maximum cross-sectional dimension.[31] Folkes and Arridge encountered these effects in their torsional measurements of the shear modulus of the highly anisotropic SBS system considered herein[7] and performed new mechanical investigations on the same specimen.[28] They found that the constraints at the two sample ends increase the shear modulus G_{SBS} for samples of length/width ratio less than about 80 compared to samples where the ratio is less than 30, by a factor of 2. This implies that, because $S_{44} = 1/G_{SBS}$, the shear compliance S_{44} depends sensitively on the sample length/width ratio as well. It is also clear that similar end effects can be expected in tensile experiments, if the length/width ratio is chosen too small.[29] Arridge and Folkes found that these effects are more pronounced along the directions of high Young moduli. From this observation they concluded that the systematic error in S_{44} should be smaller in deriving it from the tensile data, because the quantity is primarily determined by the Young moduli corresponding to off axis loading where the decay length is much less than for loading along the symmetry axis. In these experiments one determines S_{44} through the formula[7]

$$4/E_{45} = S_{11} + (2S_{13} + S_{44}) + S_{33} \qquad (15)$$

which is easily derived from eq 14. From experimental and theoretical considerations,[7] we know that $S_{11} + S_{44} \gg 2S_{13} + S_{33}$, and we can approximately write

$$4/E_{45} \approx S_{11} + S_{44} \qquad (16)$$

where E_{45} represents Young's modulus at an angle of 45° to the symmetry axis. In tensile experiments the compliance S_{11} can accurately be determined from measurements of the Young modulus perpendicular to the fiber axis. However, problems should be expected in the measurement of E_{45}, and therefore, deviations to the exact value of S_{44} are likely. This provides a plausible explanation for the discrepancy between the S_{44} value obtained from tensile experiments in ref 7 and the S_{44} value obtained from torsional experiments in refs 28 and 29, where the sample end effects have been eliminated. Taking the shear modulus of SBS at a length/width ratio larger than 120, i.e., $G_{SBS} = 0.0012$ GPa, we can calculate the "end-effect-free" shear compliance $S_{44} = 833.3 \pm 50.1$ GPa^{-1}. Since on theoretical grounds,[7] it can be shown that $S_{13} \approx 10^{-3}S_{44}$, we get $2S_{13} + S_{44} \approx 835.0 \pm 50.2$ GPa^{-1}. With this result we can now evaluate the end-effect-free compliance S_{33}' at any angle θ, whose curve is shown in Figure 8. We see that the experimental curve, corrected from end effects, is much closer to our MFE curve, the curve of Van Fo Fy and Savin, and the upper bound curve of Hashin and Hill than the noncorrected experimental curve. We also recognize that the curves of all the theoretical approaches mentioned previously lie within the error bars of the corrected experimental curve. In conclusion, this indicates that the Poisson ratio of 0.37 for the PB matrix, found by Arridge and Folkes through fitting the theoretical results to the experimental ones, might be due to end-effect errors arising in their mechanical measurements. Furthermore, in recent experimental investigations Adhikari et al.[32] have shown that the glass transition temperature of the confined PB phase is nearly identical to the glass transition temperature of the PB homopolymer. These data are also in support of a classical rubber-like behavior of the PB matrix, i.e., $\nu_{PB} \rightarrow 0.5$.

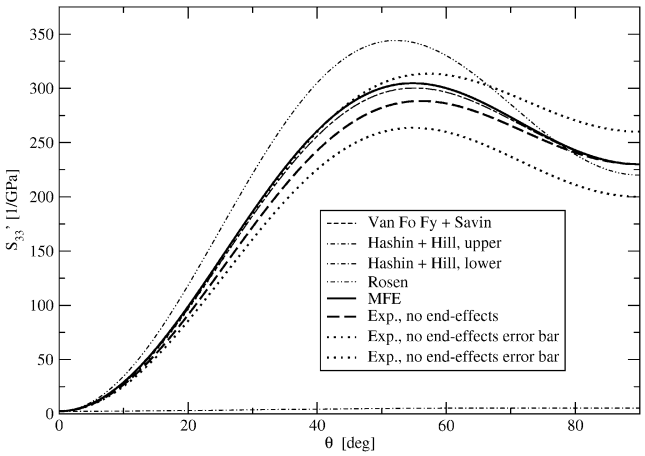

Figure 8. S_{33}' compliance yielded with the MFE method in comparison to the results obtained with the theories of fiber reinforcement and the end-effect-free experiment. The compliances S_{11} and S_{33} are adjusted to the experimental result.

5. Summary and Conclusions

In this paper we present the application of a mixed finite element method for the computation of mechanical properties of a system of hexagonally packed cylinders of polystyrene embedded in a polybutadiene matrix. The system functions as a model for the poly(styrene-butadiene-styrene) triblock copolymer at a weight fraction of 25% polystyrene. With this continuum approach we test the suitability of semiphenomenological theories of fiber reinforcement in predicting experimental elastic measurements. We find that the method of Van Fo Fy and Savin provides reliable results, which are comparable in accuracy to those of our mixed finite element approach, while the other semiphenomenological theories are shown to be less valuable. Having assessed the usefulness of these theories, we focus in a further step on the experimental measurements. We find that, within the error bars, our finite element predictions are accurate without any need for untypical assumptions for the material properties of the polybutadiene phase. Moreover, we deduce from this investigation that the accuracy of the available experimental data is not sufficient for understanding the role of the bridging chains in the linear elastic regime of this triblock copolymer. We attribute the anomalous Poisson ratio for the confined polybutadiene phase, found by Arridge and Folkes, to sample end effects manifested in their mechanical experiments. Our calculations suggest that a classical nearly incompressible rubber-like behavior of the polybutadiene phase is probable.

This work unambiguously demonstrates that a concerted improvement of experimental and theoretical techniques is necessary to gain further insight in the small-strain behavior of the poly(styrene-butadiene-styrene) triblock copolymers. From the theoretical viewpoint it is clear that a higher accuracy can only be achieved if one takes into account molecular details. Therefore, our future work will concentrate on incorporating information on a molecular level and also on exploring nonlinear behavior.

Acknowledgment. We gratefully acknowledge the financial support of this research provided by Rhodia (France) and Mitsubishi Chemical Corp. (Japan). This work was partially supported by the MRSEC Program of the National Science Foundation under Award No. PMR 00-80034.

Appendix A. Deviatoric Stress−Strain Relations

The deviatoric strain ϵ^d is defined by

$$\epsilon^d = \epsilon - (1/3)\mathbf{m}\epsilon_v \equiv (\mathbf{I} - (1/3)\mathbf{m}\mathbf{m}^T)\epsilon = \mathbf{I}_d\epsilon \quad (17)$$

where $\mathbf{I}_d$ is a deviatoric projection matrix. In isotropic elasticity the deviatoric strain is related to the deviatoric stress via the shear modulus G as

$$\boldsymbol{\sigma}^d = \mathbf{I}_d\boldsymbol{\sigma} = 2G\mathbf{I}_0\epsilon^d = 2G(\mathbf{I}_0 - (1/3)\mathbf{m}\mathbf{m}^T)\epsilon \quad (18)$$

where the diagonal matrix

$$\mathbf{I}_0 = \frac{1}{2}\begin{bmatrix} 2 & & & & & \\ & 2 & & & & \\ & & 2 & & & \\ & & & 1 & & \\ & & & & 1 & \\ & & & & & 1 \end{bmatrix} \quad (19)$$

is introduced because of the matrix notation. A deviatoric form for the elastic modulus of an isotropic material can thus be defined as

$$\mathbf{D}_d = 2G(\mathbf{I}_0 - (1/3)\mathbf{m}\mathbf{m}^T) \quad (20)$$

References and Notes

(1) Hawker, C. J.; Bosman, A. W.; Harth, E. *Chem. Rev.* **2001**, *101*, 3661.
(2) Matyjaszewski, K.; Xia, J. *Chem. Rev.* **2001**, *101*, 2921.
(3) Kaminsky, W.; Tran, P.-D.; Weingarten, U. *Macromol. Symp.* **2003**, *193*, 1; Kaminsky, W.; Albers, I.; Vathauer, M. *Des. Monomers Polym.* **2002**, *5*, 155; Kaminsky, W. *Macromol. Symp.* **2001**, *174*, 269.
(4) Moad, G.; Mayadunne, R. T. A.; Rizzardo, E.; Skidmore, M.; Thang, S. H. *Macromol. Symp.* **2003**, *192*, 1.
(5) Folkes, M. J.; Keller, A. In *Block and graft copolymers*; Burke, J. J., Weiss, V., Eds.; Syracuse University Press: Syracuse, NY, 1973; p 87.
(6) Folkes, M. J.; Keller, A. *Polymer* **1971**, *12*, 222.
(7) Arridge, R. G. C.; Folkes, M. J. *J. Phys. D: Appl. Phys.* **1972**, *5*, 344.
(8) Odell, J. A.; Keller, A. *Polym. Eng. Sci.* **1977**, *17*, 8.
(9) Allan, P.; Arridge, R. G. C.; Ehtaiatkar, F.; Folkes, M. J. *J. Phys. D: Appl. Phys.* **1991**, *24*, 1381.
(10) Zienkiewicz, O. C.; Taylor, R. L. *The finite element method, volume 1: the basis*; Butterworth-Heinemann: Oxford, 2000.
(11) Malvern, L. E. *Introduction to the mechanics of a continuous medium*; Prentice Hall: Englewood Cliffs, NJ, 1969.
(12) We use the matrix notation, in which the second-ranked symmetric tensors are represented by six-dimensional vectors with the components related according to the rules 1 ⇔ 11, 2 ⇔ 22, 3 ⇔ 33, 4 ⇔ 23, 5 ⇔ 31, and 6 ⇔ 12, whereas for the representation of the fourth-ranked tensors (elastic constants, elastic compliances, etc.) we use 6 × 6 matrices with the components related as 11 ⇔ 1111, 23 ⇔ 2233, 46 ⇔ 2312, etc. The relations are exact for the coefficients of the stress tensor and the tensor of elastic constants, and usual additional factors of 2 and 4 are needed for the strain and compliance tensors.
(13) Gusev, A. A. *J. Mech. Phys. Solids* **1997**, *45*, 1449.
(14) Gusev, A. A. *Macromolecules* **2001**, *34*, 3081.
(15) Takayanagi, M.; Harima, H.; Iwata, Y. *Mem. Fac. Eng., Kyushu Univ.* **1963**, *23*, 1.
(16) Whitney, J. M.; Riley, M. B. *Am. Inst. Aeronaut. Astronaut. J.* **1966**, *4*, 1537.
(17) Hashin, Z. *J. Mech. Phys. Solids* **1965**, *13*, 119.
(18) Hill, R. *J. Mech. Phys. Solids* **1964**, *12*, 199.
(19) Hashin, Z.; Rosen, B. W. *Trans. ASME* **1964**, *31*, 223.
(20) Rosen, B. W. *Proc. R. Soc. London* **1970**, *A319*, 79.
(21) Van Fo Fy, G. A.; Savin, G. N. *Polym. Mech.* **1965**, *1*, 106.
(22) Chamis, C. C.; Sendeckyj, G. P. *J. Compos. Mater.* **1968**, *2*, 332.
(23) Fetters, L. J.; Lohse, D. J.; Graessley, W. W. *J. Polym. Sci., B: Polym. Phys.* **1999**, *37*, 1023.

(24) Gent, A. N. *Engineering with rubber: how to design rubber components*; Carl Hanser: Munich, 2001.
(25) Rudd, J. F. In *Polymer handbook*; Brandrup, J., Immergut; E. H., Eds.; Wiley: New York, 1989; V/81.
(26) van Krevelen, D. W. *Properties of polymers*; Elsevier: Amsterdam, 1990.
(27) Gilmour, I.; Trainor, A.; Haward, R. N. *J. Polym. Sci.: Polym. Phys. Ed.* **1974**, *12*, 1939.
(28) Folkes, M. J.; Arridge R. G. C. *J. Phys. D: Appl. Phys.* **1975**, *8*, 1053.
(29) Arridge, R. G. C.; Folkes, M. J. *Polymer* **1976**, *17*, 495.
(30) Arridge, R. G. C.; Barham, P. J.; Farrell, C. J.; Keller, A. *J. Mater. Sci.* **1976**, *11*, 788.
(31) Horgan, C. O. *J. Elasticity* **1972**, *2*, 169, 335; *Int. J. Solids Struct.* **1974**, *10*, 837.
(32) Adhikari, R.; Michler, G. H.; An Huy, T.; Ivan'kova, E.; Godehardt, R.; Lebek, W.; Knoll, K. *Macromol. Chem. Phys.* **2003**, *204*, 488.

MA035528D